Buoy geometry and its influence on survivability for a point absorbing wave energy converter: Scale experiment and CFD simulations

Engström, J; Sjökvist, L; Göteman, M; Eriksson, M; Hann, M; Ransley, EJ; Greaves, D; Leijon, M

Published in:
Default journal

Publication date:
2017

Buoy geometry and its influence on survivability for a point absorbing wave energy converter: Scale experiment and CFD simulations

Jens Engström[†]
Uppsala University
Uppsala, Sweden

Linnea Sjökvist[†*]
Uppsala University
Uppsala, Sweden

Malin Göteman
Uppsala University
Uppsala, Sweden

Mikael Eriksson
Uppsala University
Uppsala, Sweden

Martyn Hann
Plymouth University
Plymouth, UK

Edward Ransley
Plymouth University
Plymouth, UK

Deborah Greaves
Plymouth University
Plymouth, UK

Mats Leijon
Uppsala University
Uppsala, Sweden

[†]First authors
[*]Corresponding author: linnea.sjokvist@angstrom.uu.se

1. INTROCUCTION

For wave energy to be an economically viable energy source, the technology has to withstand power levels during storms that can be close to 50 times higher than during normal operating conditions [1], and withstand many years of wear. The impact of high wave loads is studied not only within the field of wave energy, but has long been a subject of study for ships, platforms and other offshore structures.

To model the force on the device under extreme and/or overtopping waves is a difficult task. Experiments are expensive and difficult to implement, and numerical methods are either very computationally demanding CFD-methods, or less accurate approximative methods. In addition, the performance and experienced forces during extreme waves are model dependent, and different offshore structures must be studied independently.

Here, a 1:20 scale model of the Uppsala University point-absorber type wave energy converter (WEC) [2] has been tested in extreme wave conditions at the COAST Laboratory Ocean Basin at Plymouth University. The WEC consists of a linear generator connected to a buoy at the sea surface, and performance of two different buoys is studied: a cylinder and cylinder with moonpool. Two types of wave sets have been used: focused waves embedded into regular waves, and irregular waves.

In [3], the line forces measured in the experiment were studied, since this is a parameter of high relevance for device survivability. The focus of this paper is on comparing the performance of the two buoys, and on analysing the experimental data using a numerical model. A fully non-linear computational fluid dynamics (CFD) model based on OpenFOAM is presented and validated.

2. METHOD

2.1 Experimental setup

2.1.1 Model

The scale model is based on the point-absorber WEC developed at Uppsala University [2]. In the 1:20 model used in the experiment the generator damping is simplified by friction damping, exerted by Teflon blocks applying force to the vertical sides of the translator, see Figure 1. Two buoys were tested; the first is a regular vertical cylinder (CYL) and the second is a vertical cylinder with moonpool (CWM). The dimensions of the buoys were chosen to give comparable waterplane area. In full scale, the diameter of the CYL and CWM buoys are 3.4 m and 4 m, and their masses are 5736 kg and 8592 kg, respectively, and the translator mass is 6240 kg. The remaining physical parameters can be found in [3], where the experiment is described in more detail. Since one of the aims of this project is to provide design criteria for offshore survivability under extreme weather conditions, all values are presented in full scale.

2.1.2 Waves

Extreme wave events are surface gravity waves whose wave heights are much larger than expected for a given

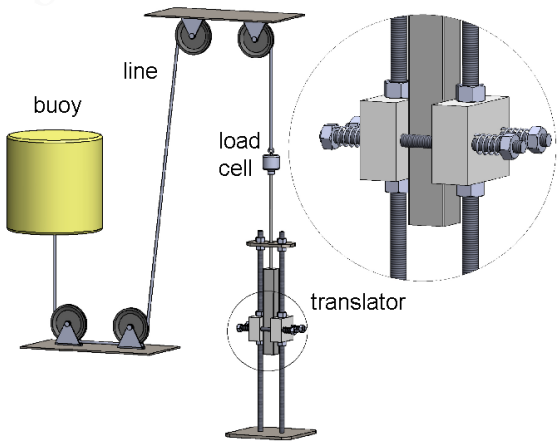

Figure 1: The 1:20 model used in experiment.

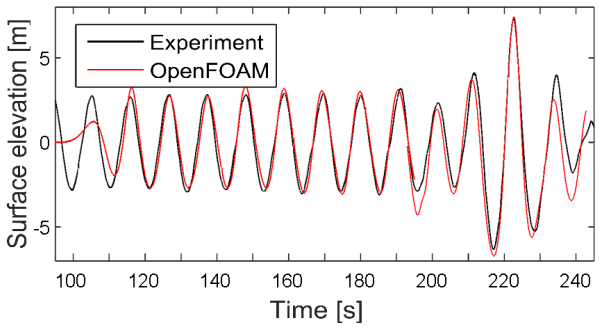

Figure 2: The incident wave simulated in OpenFOAM is compared to the experimental wave.

sea state. When measuring survivability of offshore structures, it is common to discuss extreme waves with certain statistical return periods at a specific location. An 80-year return period sea state at the Wave Hub site was chosen for these measurements. To represent extreme wave loading on the device, focused wave events have been embedded in regular wave backgrounds with a range of 32 different periods and different phase positions of the embedded focused wave [4]. The background wave period was ranged between 10.0 s and 13.7 s, and the wave height was 7.2 m. The input for the physical wave paddles for the embedded focused waves is derived using the NewWave formulation [5].

In addition, two irregular wave sets were run to obtain the system's response in realistic operating conditions. The irregular waves were based on a JONSWAP spectrum and run for 67 min (full scale). The significant wave height for the two irregular waves was 7.2 m and 7.4 m, the maximal wave height 12.9 m and 11.7 m, and the energy period 13.4 s and 14.0 s, respectively.

2.1.3 Measurements

The wave tank measures 35 x 15.5 m and is equipped with 24 flap type paddles. Line force was measured by a miniature low profile load cell, attached to the top of the translator, see Figure 1. Motion capture of the buoy was performed via an optical Qualisys system, synchronized with the load cell at a sampling frequency of 128 Hz.

2.2 Numerical simulations

The WEC has been simulated in the open source software OpenFOAM. For engineering usability, all simulations were performed in full scale. The simulations are made in 3D, and a moving mesh is used. The OpenFOAM model is solved using the two-phase Navier-Stokes solver interDyMFoam, and the turbulence is modeled using the Reynolds-Average Navier-Stokes (RANS) approach with a RNG k-ε turbulence model. The numerical wavetank was 300 m long, 100 m high and had a width of 60 m, the water depth was 50 m. It was discretized using 800000 hexahedral mesh elements. The waves in the model are generated and absorbed using the library waves2Foam. The simulations were performed in two separate wave events: first 100 s of monochromatic waves, and then 50 s of an extreme wave event, which was a superposition of the four most significant wave frequencies of the experimental wave. The simulated wave is compared to the experimental wave in Figure 2.

The WEC was simulated as a floating buoy with six degrees of freedom, restrained by a force, F_{line}, directed along a unit vector from the buoy to a fixed position on the seabed, $\hat{r}$. The equation of motion for the floating buoy is described by

$$(m_b + m_t)\ddot{\bar{r}}(t) = \iint p\hat{n}dS - F_{\text{line}}\hat{r} - m_b\bar{g} \qquad (1)$$

where m_b and m_t are the mass of the buoy and of the translator, $\bar{r}$ is the position vector of the buoy, and p is the water pressure. As long as the line is not slack, the restraining forces on the buoy are given by

$$F_{\text{line}}\hat{r} = \bar{F}_{\text{grav}} + \bar{F}_{\text{PTO}} + \bar{F}_{\text{spring}} \qquad (2)$$

where the gravity force on the translator is $\bar{F}_{\text{grav}} = m_t g\hat{r}$, the generator damping is $\bar{F}_{\text{PTO}} = \gamma\dot{r}_t\hat{r}$ and the translator has a limited stroke length governed by the endstop spring force $\bar{F}_{\text{spring}} = \kappa l_\kappa \delta_{\text{up}}\hat{r}$. If the line is slack, F_{line} is zero. A more thorough description of the numerical model is given in [6].

In the experiment presented in this paper, no PTO-damping was applied. In the simulation, instead a damping of 5 kNs/m was applied, to model the mechanical losses in the system. When the endstop spring was hit, the elasticity of the connection line (300 kN/m in full scale) is relevant and was included in the model.

3. RESULTS

3.1 Validation of the numerical model

The wave elevation of the numerical model agrees well with the experimental wave, as can be seen in Figure 2. The buoy motion in surge and heave for both buoys is shown in Figure 3. As can be seen in the figure, the heave positions from the simulations coincide well with the experimental results. The surge motion is slightly underestimated by the OpenFOAM model, but the pattern with larger surge excursions for the CYL is clearly visible and of the same magnitude. It is suggested that the underestimated surge motion can be

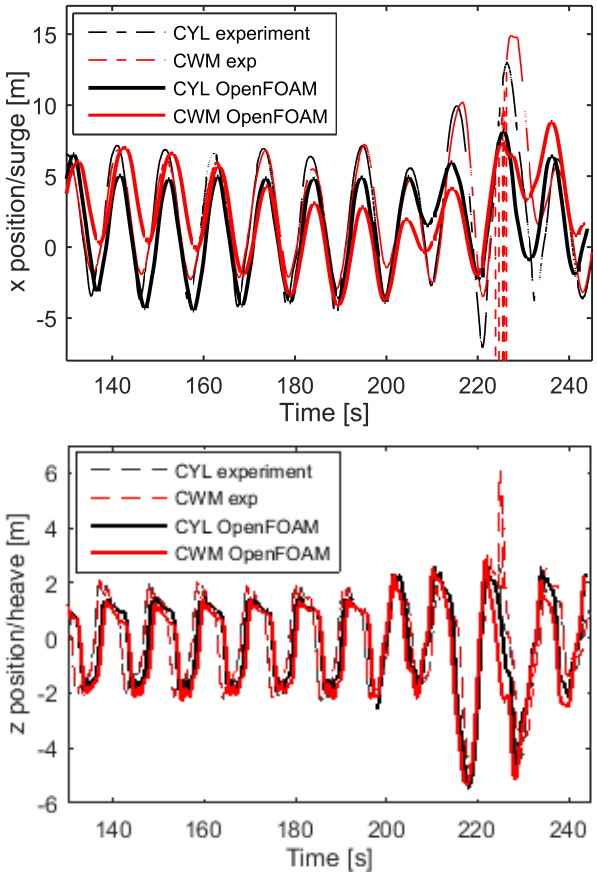

Figure 3: Surge and heave position from OpenFOAM simulations and experiments for the regular embedded focus wave.

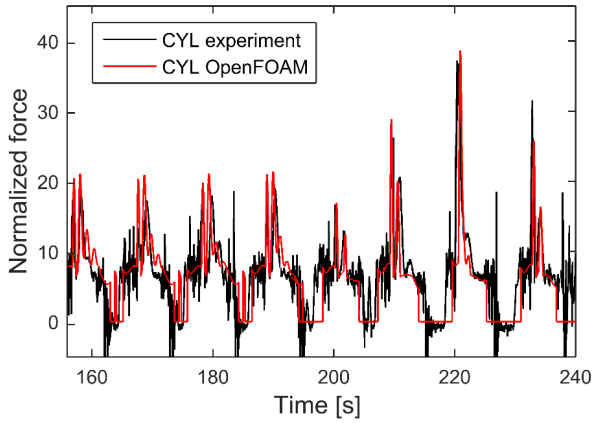

Figure 4: Normalized force. OpenFOAM simulation vs. experiment for the CYL buoy.

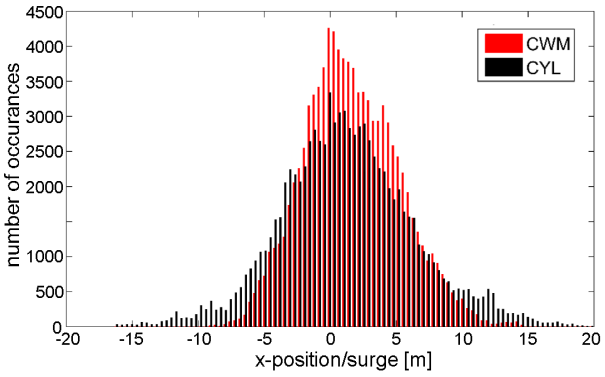

Figure 5: Surge deviation in irregular waves.

partly attributed to the fact that the model neglects the line elasticity unless the endstop spring was hit.

The line force was simulated, and compared with the experimental force in Figure 4 for the CYL buoy. The force is normalized by the buoyancy force according to $F = (F_{\text{line}} - m_t g)/\rho g V$, where V is the submerged volume of the buoy at equilibrium. The simulated force agrees well with the experimental data, for both the monochromatic waves and the extreme wave. The agreement for the CWM buoy is also good, but the figure has been omitted due to page limitations.

3.2 Comparison between the two buoys

3.2.1 Buoy dynamics

The surge and heave motion in regular and embedded extreme wave for the two buoys is shown in Figure 3. In heave motion, the motion of the two buoys are more or less equal and is limited by the stroke length of the device; the translator hits the upper end stop spring in each wave cycle.

To minimize wear on the connection line and reduce maintenance costs of the WEC, a small surge motion is desirable for this type of WEC [7]. In Figure 3 it can be seen that except for a few instances, the CYL has larger excursions in surge, despite its slightly smaller vertical cross section. To analyse this in a qualitative setting, the surge deviation for irregular waves is shown in Figure 5. For this 67 min time-series of irregular waves, the CYL buoy shows a clear tendency for larger surge excursions. For the second irregular wave set, the result is the same, but the tendency is weaker. The maximal surge deviation corresponds to an inclination angle of 15° between the generator and the buoy, which can be compared to full scale experiments where a maximal angle of 8° was measured [7].

3.2.2 Line force

Conclusions on which buoy gives rise to the highest line forces are more difficult to draw. In the irregular wave tests, the CYL buoy shows a tendency to be subjected to higher forces, as shown in Figure 6. The data is presented using a Gaussian distribution in order to clarify trends, and the measured line force is normalized with the buoyancy as discussed above. However, the tendency for higher line forces for the CYL buoy cannot be seen in the 32 embedded focused wave tests; in some of the tests the CWM experiences higher forces.

There is a large spread among the force measurements that adds to the uncertainty of the conclusions regarding line force, which has been discussed by the authors in [3]. Nevertheless, due to the consistent result in both long

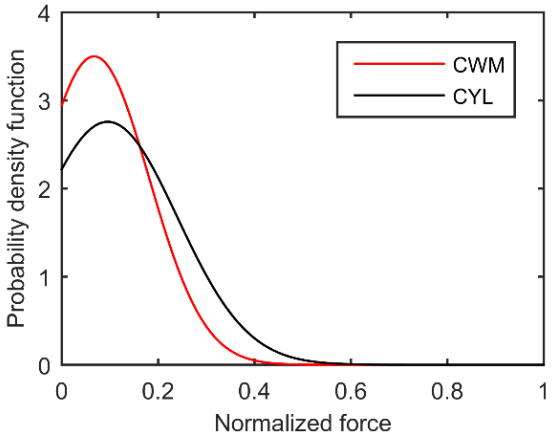

Figure 6: The Gaussian distribution of the line force for the two buoys in irregular waves.

time-series of irregular wave tests, a cautious conclusion can be drawn that the CYL experiences a larger number of high line forces during realistic irregular waves.

3.2.3 *Turbulence*

Turbulence in moonpools may affect the dynamics of the buoys [8]. To study this, the magnitude of the turbulent kinetic energy in the vicinity of the two buoys has been plotted in Figure 7 at the time step where the surge velocity is maximum. It can be seen that the turbulence inside the moonpool is lower than just outside, and the largest turbulence is found on the water surface outside the buoy, downstream of the wave direction. It is also seen that the turbulence in the vicinity of the CWM buoy is not larger than in the vicinity of the CYL, implying that the larger excursions in surge motion does not derive from turbulence in the moonpool.

4. CONCLUSIONS

The dynamics of two different buoy types has been compared when subjected to 1:20 tests in extreme wave conditions. A line force normalized by the buoyancy force was considered to enable a more fair comparison between the buoys. The cylinder with moonpool has less excursion in surge, which is a desired behavior for this type of point absorbing WEC since it decreases the inclination angle and thus the wear on the line. The cylinder shows some tendency for a larger number of high forces in irregular waves, but this was not seen in all of the embedded focused wave tests. The OpenFOAM simulation model compares well with experimental data both for buoy position and line force. Using the simulation tool, it was found that the larger surge deviation does not derive from turbulence in the moonpool.

5. ACKNOWLEDGEMENTS

This research is supported by StandUp for Energy, Centre for Natural Disaster Science in Sweden, Carl Tryggers Stiftelse, the Swedish Energy Agency, VR (grant 2015-04657), Bengt Ingeströms fund, Wallenius foundation, and Miljöfonden. The computations were performed on resources provided by the Swedish National Infrastructure for Computing (SNIC) at UPPMAX.

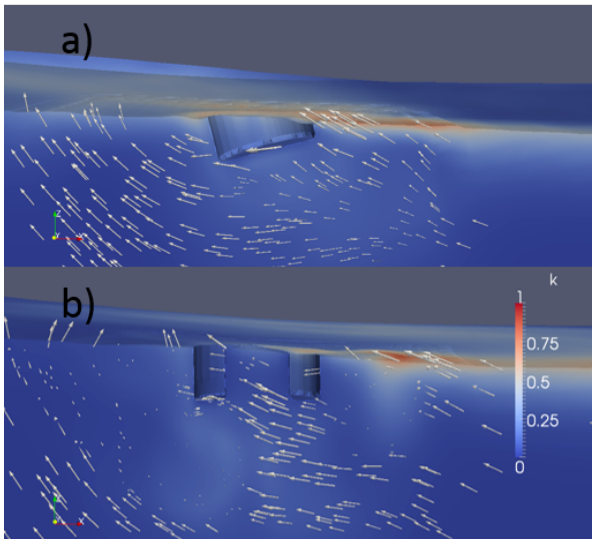

Figure 7: Simulation of turbulence around the a) CYL and b) CWM buoy. The magnitude of the turbulent kinetic energy is seen as color, while the arrows show the water velocity.

6. REFERENCES

[1] Waters, R., Engström, J., Isberg, J., and Leijon, M., 2009. "Wave climate off the swedish west coast". *Renewable Energy,* ***34***(6), pp. 1600–1606.

[2] Eriksson, M., Waters, R., Svensson, O., Isberg, J., and Leijon, M., 2007. "Wave power absorption: Experiments in open sea and simulation". *Journal of Applied Physics,* ***102***(8), p. 084910.

[3] Göteman, M., Engström, J., Eriksson, M., Hann, M., Ransley, E., Greaves, D., and Leijon, M., 2015. "Wave loads on a point-absorbing wave energy device in extreme waves". *Journal of Ocean and Wind Energy,* ***2***, pp. 176–181.

[4] Bennett, S., Hudson, D., and Temarel, P., 2012. "A comparison of abnormal wave generation techniques for experimental modelling of abnormal wave–vessel interactions". *Ocean Engineering,* ***51***, pp. 34–48.

[5] Ransley, E., Hann, M., Greaves, D., Raby, A., and Simmonds, D., 2013. "Numerical and physical modelling of extreme wave impacts on a fixed truncated circular cylinder". In Proc 10th Eur Wave Tidal Energy Conf (EWTEC), Aalborg, Denmark.

[6] Sjökvist, L., Wu, J., Engström, J., Eriksson, M., and Göteman, M., 2017. "Numerical models for the motion and forces of point-absorbing wave energy converters in non-linear waves". *submitted to Ocean Engineering.*

[7] Savin, A., Svensson, O., and Leijon, M., 2012. "Azimuth-inclination angles and snatch load on a tight mooring system". *Ocean Eng.,* ***40***, pp. 40–49.

[8] Fredriksen, A., Kristiansen, T., and Faltinsen, O., 2014. "Experimental and numerical investigation of wave resonance in moonpools at low forward speed". *Applied Ocean Research,* ***47***, pp. 28–46.